Optimization of the Memory Weighting Function in Stochastic Functional Self-Organized Sorting Performed by a Team of Autonomous Mobile Agents

Sorinel Adrian Oprisan[*]

Department of Psychology,
University of New Orleans,
New Orleans, LA 70148

The activity of a team of autonomous mobile agents formed by identical "robot-like-ant" individuals capable of performing a random walk through an environment that are able to recognize and move different "objects" is modeled. The emergent desired behavior is a distributed sorting and clustering based only on local information and a memory register that records the past objects encountered. An optimum weighting function for the memory registers is theoretically derived. The optimum time-dependent weighting function allows sorting and clustering of the randomly distributed objects in the shortest time. By maximizing the average speed of a texture feature (the contrast) we check the central assumption, the intermediate steady-states hypothesis, of our theoretical result. It is proved that the algorithm optimization based on maximum speed variation of the contrast feature gives relationships similar to the theoretically derived annealing law.

1. Introduction

Self-organization was originally introduced in the context of physics and chemistry to describe how microscopic processes give rise to macroscopic structures in out-of-equilibrium systems [1]. Recently, this concept was extended to ethnology to provide a concise description of a wide range of collective phenomena in animals, especially in social insects. This description does not rely on individual complexity to account for complex spatio-temporal features, which emerge at the colony level, but rather assumes that interactions among simple individuals can produce highly structured collective behaviors. The rules specifying the interactions among the constituent units of the system are executed based on purely local information, without reference to the global pattern, which is an emergent property of the system.

---

[*]Electronic mail address: soprisan@uno.edu.

Self-organization can, at least partially, describe the collective activities of social insects, including the formation of trail networks and foraging patterns in many ant species [2–5], rhythmical patterns of activity in ants (Leptothorax) [6, 7], thermoregulation in clusters of bees [8], the piling of dead bodies by ants (Pheidole) [9], larval sorting by ants (Leptothorax) [9], or the dynamics of colony development in wasps (Polistes) [10]. Self-organization has also been applied to modeling social organization, including hierarchical differentiation [11–13], division of labor [13, 14], and age (or temporal) polyethism [15].

At a time when the world is growing so complex that no single human being can understand it; when information, and not the lack of it, threatens our lives; when users can no longer master bloated software, swarm intelligence offers an alternative way of designing computing systems. In swarms, autonomy, emergence, and distributed functioning replace control, preprogramming, and centralization.

There has been an upsurge of interest in swarm-based robotics in recent years [16] as it provides an interesting alternative to more classical approaches in robotics. Some tasks may be inherently too complex or impossible for a single robot to perform. A swarm of simple robots may also be more flexible without needing to reprogram the robots, and more reliable and fault-tolerant because one or several robots may fail without affecting task completion. Furthermore, theories of self-organization teach us that randomness or fluctuations in individual behavior, far from being harmful, may in fact greatly enhance the ability of the system to explore new behaviors and new solutions. In addition, self-organization and decentralization, together with the idea that interactions among agents need not be direct but can rather take place through the environment, point to the possibility of significantly reducing communications between robots. Also, central control is usually not well suited for dealing with a large number of agents, not only because of the need for robot-to-controller-and-back communications, but also because failure of the controller implies failure of the whole system.

For modeling and simulation of swarm intelligence inspired by insect societies many different approaches are possible. On one side the complete group can be seen as one system and the variation of its parameter can be modeled on the macro level. This paradigm yields several disadvantages. The most important are that no variations in the behavior of the individual can be considered and that differences in the spatial structure of the entities' environment cannot influence their behavior [17]. Other forms of modeling societies generate the collective behavior from "bottom up." Different mathematical micro-simulation approaches result in large equation systems, for example, modeling *via* decision matrices or stochastic processes, thus individual or spatial variations can hardly be incorporated, see [16] or [18]. On the other hand modeling societies based on cellular automata (CA) or multi-agent sys-

tems enables the researcher to specify the local behavior of the individual spatial unit or entity. Simulating the actions of the individuals directly reproduces the behavior of the complete system. As our research focus is on the behavior and interaction of individual entities and not on a special spatial pattern (like, for example, in [19]), we decided to use multi-agent simulation.

The mission of the robots is to search and collect "food-items" in a foraging area and sort them into disjoint piles. In this paper a theoretical expression for the time-dependent memory radius r for the functional self-organization process [20–24] is derived. The basis of the optimization is the assumption of intermediate steady states of the aggregation process. The global contrast feature monitors the degree of aggregation.

This article is organized as follows. Section 2 puts stochastic functional self-organization in context by describing the environment and the local rules governing the dynamics of the mobile agents. Section 3 is dedicated, in its first part, to the theoretical derivation of the time-dependent memory radius in order to attain a final sorting stage in the shortest possible time. The second part of section 3 implements the control strategy based on the global feature (contrast). The computation of the iteration time steps for a specific value of optimal memory radius confirms the theoretical relationship derived in the first part of section 3. Section 4 is dedicated to discussing the main results and indicating directions for further research. We also highlight some different approaches to artificial intelligence based on a centralized controller. A mathematical appendix provides theoretical insight on the limit values of the global measure (contrast feature).

2. The mechanism of stochastic functional self-organization

There is an increasing interest in CA models of physical phenomena due to the simplicity of computational tasks and the great flexibility of the models [25–28].

Our model is based on the following assumptions.

1. The environment is a two-dimensional toroidal lattice with $N_x \times N_y$ sites. The periodic lattice (torus) was considered in order to eliminate the finite size effects.

2. The lattice sites are occupied by *objects* denoted with the letters a, b, c, and so on. A *free site* is said to be occupied by a ϕ-type object.

3. Throughout the environment some *entities* (robot or robot-like-ant (RLA)) perform a random walk like motion. At any moment, a robot carries an object. A robot carrying a ϕ-type object is a *free robot*. The robots move randomly through the lattice, only one robot being allowed at one site.

4. When a robot moves to a given site it must decide if there are conditions to put down the object being carried and to pick up the existing one.

The swapping condition writes

$$f_\alpha \geq f_\beta, \tag{1}$$

where f_α is the weighted frequency of the carried α-type object and f_β is the weighted frequency of the encountered β-type object. Every RLA records in its memory a binary string with the following structure:

$$s_{\alpha,\tau} : u_{\alpha,1} u_{\alpha,2} \ldots u_{\alpha,\tau}, \tag{2}$$

where

$$u_{\alpha,i} = \begin{cases} 1 & \text{if an } \alpha\text{-type object was encountered at step } i, \\ 0 & \text{otherwise.} \end{cases} \tag{3}$$

Based on equations (2) and (3) the following conservation rules take place $\sum_{i=1}^{\tau} u_{\alpha,i} = n_\alpha$, for any $\alpha = \overline{1, T}$, where n_α is the total number of α-type objects encountered and $\sum_{\alpha=1}^{T} u_{\alpha,i} = 1$, for any $i = \overline{1, \tau}$, where T is the total number of distinct object types.

There are few distinct approaches regarding the weighting function. One important class was proposed by Deneubourg in [9] and consists of a memory register of fixed length with equal weight. As time passes the older (less significant) record is deleted, all the other records are shifted one location, and the new record is entered on the first (most significant) place. Another important class of weighting functions was proposed in [20–23] and uses a first order recurrence to define the actual state of the CA. The main advantage of such a weighting function is its computational efficiency and long (temporal) correlation. The computational efficiency means that to compute the actual state of the CA we only need two real variables: the previous state of the CA and the state associated with the newly encountered object type. For higher order recurrence the number of state variables increases but is still small compared to the shift register like memory. Long (temporal) correlation means that the actual state of the recursively defined weighted function depends on the history of the system states and not on an arbitrarily truncated record. As was proved in [20, 21, 24] there is an intrinsic limit of the temporal correlation imposed by machine accuracy. However, the temporal length of correlation for the model we proposed is a few orders of magnitude bigger than for the fixed number of shift register like memory.

In our approach of mobile agents self-organization, every object type is characterized at any instant τ by a weighted frequency:

$$f_\alpha(\tau) = \frac{\sum_{i=1}^{\tau} w(i) u_{\alpha,i}}{\sum_{i=1}^{\tau} w(i)}, \tag{4}$$

where $w(i)$ is an appropriate weighting function. The weighting function is

$$w(i) = \frac{1}{r^{i-1}}, \tag{5}$$

which indicates that if $r \gg 1$, then the contribution of the step τ (with $\tau \gg 1$) to the present decision is quite insignificant and we have a *short-type memory*. This choice simulates the long term or remnant memory effect. The limit case $r = 1$ corresponds to an infinite length memory with equally weighted records or equivalent temporal positions. When $r < 1$ then it exacerbates the contribution of the τ steps with $\tau \gg 1$ and diminishes the contribution of the most recent ones [22, 23]. This type of memory function that enhances the effect of past history was suggested as a possible mechanism for microscopic models of metastasis [21, 22, 24]. In our simulations $r > 1$. From equations (4) and (5) one obtains

$$f_\alpha(K) = r^{K-1} \frac{r-1}{r^K - 1} \sum_{i=1}^{K} \frac{u_{\alpha,i}}{r^{i-1}}, \tag{6}$$

which represents the weighted measure of α-type objects after K steps through the lattice. As can be seen from the above formula, two successive weighted measures $f_\alpha(K)$ and $f_\alpha(K+1)$ are related through a first order recurrence. In our particular choice of the weighting function (see equation (5)), a shift in the record with one step to allow a new entry is given by dividing the old value of the weighted measure through the memory radius r and adding the new entry.

Extensive numerical simulations indicate that the memory radius r should depend on the cluster dimension (i.e., aggregation stage) in order to optimize the computational effort [20, 21]. Therefore, to obtain an optimum computational time a simulated annealing in respect to the memory radius must be carried out. Conclusions based on many simulations showed that clustering processes occur for any $r > 1$ and that the speed with which the system reaches a sorted steady state depends sensibly on r (see Figure 1). This situation is similar with one encountered in annealing processes where a proper temperature decreasing law must be chosen in order to anneal a piece of steel in the shortest time without any internal stress accumulation. In our model, a very fast annealing (decreasing the memory radius) drives the system into an equilibrium state consisting of many small clusters (nonequilibrium state). The system cannot continue to sort the objects by itself without a random input or a proper, time dependent, memory radius. Our main goal in this study is to derive a theoretical expression for the time-dependent memory radius r. An appropriate numerical test is performed to check the findings in order to minimize the computational time required to achieve a global sorting steady state.
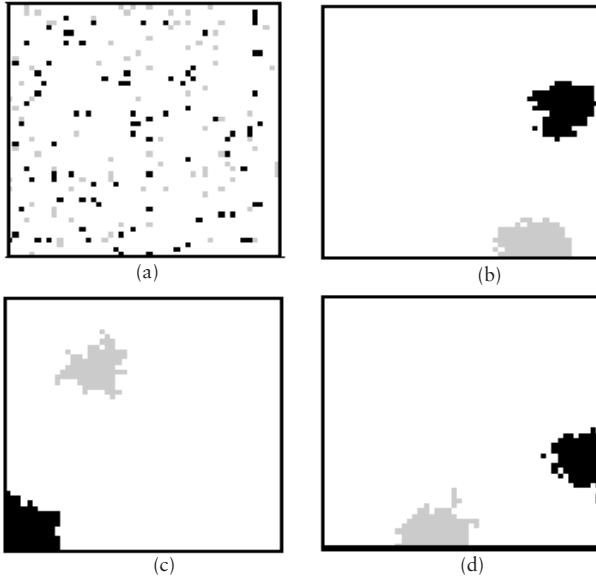
Figure 1. The statistical average of the aggregation time strongly depends on the memory radius r. Starting with an arbitrary initial configuration (a) and with 30 RLA, $N_a = 100, N_b = 100$, in a 50×50 two-dimensional toroidal lattice, clusters appear for $r = 1.1$ after 2.5×10^5 steps (b), $r = 1.3$ after 6.5×10^5 steps (c), and $r = 1.5$ after 10^6 steps (d). Extensive numerical simulations suggested the idea that an appropriate time-dependent memory radius can optimize the algorithm.

3. The results

3.1 Analytic relationship between memory radius and aggregation stage based on intermediate steady states hypothesis

Let us add a new index n, the discrete (computational) time step, to the swapping condition of equation (1). Let us analyze the case when after n time steps the swapping condition is not fulfilled but it turns out to be true at step $n + 1$, namely:

$$f_\alpha^n < f_\beta^n \tag{7a}$$
$$f_\alpha^{n+1} > f_\beta^{n+1}. \tag{7b}$$

To emphasize the main idea, only two object types were considered on the lattice. Using equation (3) we may write $u_{\beta,i}^n = 1 - u_{\alpha,i}^n$, and

$$f_\beta^n = \sum_{i=0}^{\tau} \frac{u_{\beta,i}^n}{r^i} = \sum_{i=0}^{\tau} \frac{1}{r^i} - f_\alpha^n. \tag{8}$$

Substituting equation (8) into equation (7a) results in

$$f_\alpha^n < \frac{1}{2} \sum_{i=0}^{\tau} \frac{1}{r^i}.$$

The only way to fulfill the swapping condition after $n + 1$ time steps is to add the bit "1" to the most recent entry in the binary string (equation (2)) of the α-type object. Using equation (6), the swapping condition writes

$$f_\alpha^n > r\left(\frac{1}{2} \sum_{i=0}^{\tau} \frac{1}{r^i} - 1 \right),$$

where the following recurrent relationship was used:

$$f_\alpha^{n+1} = 1 + \frac{1}{r} f_\alpha^n.$$

Summarizing, in the limit of large memory $\tau \to \infty$ the swapping conditions of equation (7) write

$$\frac{r(2 - r)}{2(r - 1)} < f_\alpha^n < \frac{r}{2(r - 1)}. \tag{9}$$

One can imagine that the aggregation process takes place progressively. Namely, in a first stage, starting with a random distribution of the objects, the RLAs form only two-object clusters, then they form only three-object clusters, and so forth. This *intermediate steady states assumption* helps us to establish a quantitative relationship between the memory radius r and the aggregation stage. Thus, a two-object cluster appears, at the time step n, if the binary string of the α-type object writes $100\ldots$, and, therefore, the swapping condition that ensures two-object clusters aggregation, see equation (9), gives $r \in (2^{1/2}, 2)$. In the same way, the most probable binary string in a fully sorted environment with clusters composed only of two objects is $1100\ldots$ and, therefore, the swapping condition of equation (7) reduces to $r \in (r^{1/3}, r^{1/2})$. Generally, it is straightforward that transition from a p-object clusters steady state to $(p + 1)$-object clusters requires $r \in (2^{1/(p+1)}, 2^{1/p})$.

The question is: How long will it take, in conventional iteration steps, to realize a complete two-object clusters steady state and then a three-object one and so on? To answer this question, let us denote by N_α the number of α-type objects in the lattice and with $\sqrt{N}$ the linear dimension of the square lattice we considered. A uniform distribution of the objects in the lattice implies a mean distance λ between the same object types given by the conservation condition

$$N_\alpha = \left(1 + \frac{\sqrt{N}}{\lambda} \right)^2,$$

which implies

$$\lambda = \frac{\sqrt{N}}{2} \frac{1 + \sqrt{4N_\alpha - 3}}{N_\alpha - 1}.$$

During the aggregation process the mean-free distance between the objects increases due to the decreasing number of clusters. We propose, as a conventional iteration time step needed to switch between p and $p+1$-objects steady clusters, a quantity proportional with the sum of the corresponding mean-free distance between the clusters. For example,

$$\lambda^{1\to2} = \frac{\sqrt{N}}{2} \sum_{i=N_\alpha/2}^{N_\alpha} \frac{1}{\sqrt{4i - 1} - 1},$$

where the superscript $1 \to 2$ designates the initial and, respectively, final aggregation steady states. The proportionality constant depends on the successive identical steps required to visit the same cluster in order to transport them to their nearest neighbors. Therefore, taking into account this successive (minimal) number of repetitive visits, the above relation can be generalized as

$$\lambda^{k\to k+1} = (2k + 1)\frac{\sqrt{N}}{2} \sum_{i=N_\alpha/(k+1)}^{\frac{N_\alpha}{k}} \frac{1}{\sqrt{4i - 1} - 1}. \tag{10}$$

Figure 2 shows the relationship between the necessary simulation time steps and the intermediate steady states for different concentrations of the objects. This plot suggests that, with a constant value of the memory radius r small clusters with dimension less than 10 appear very quickly. After that, there is a saturation process that takes place due to uncorrelated activities of the RLAs and the sorting process slows down. The number of iteration steps to reach a given intermediate steady state seems to be proportional to the concentration of the objects. On the other hand, we observed that for every steady state (cluster dimension p) there is an optimum value of the memory radius r. Therefore, by eliminating the steady state cluster dimension between the memory radius and time steps, some insight can be obtained concerning the relationship between the memory radius and time step (see Figure 3). The plot suggests that, for a fixed concentration, there is a domain of allowed memory radius values r that result in a global sorting. However, inside the shadowed area there are infinitely different time (step)-dependent memory radius relationships. Our goal is to identify the path that leads to the global steady state in the shortest time.

Replacing the sum from equation (10) by

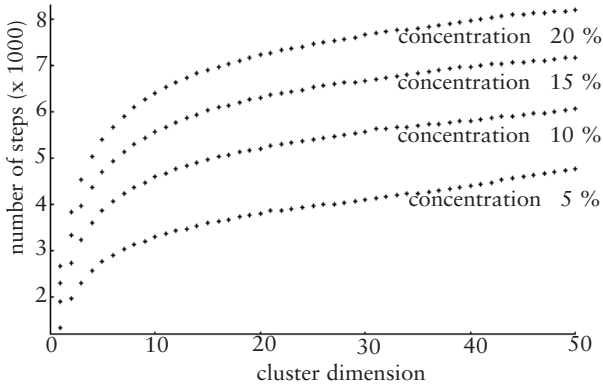$$\sum_{i=N_\alpha/(k+1)}^{N_\alpha/k} \frac{1}{\sqrt{4i}},$$

Figure 2. The plot of required iteration steps against the cluster dimension for a fixed concentration of objects into the lattice reveals a linear relationship between the computation time and the concentration. The environment was a rectangular 100×100 lattice containing only two object types and one RLA, memory radius $r = 1.1$.
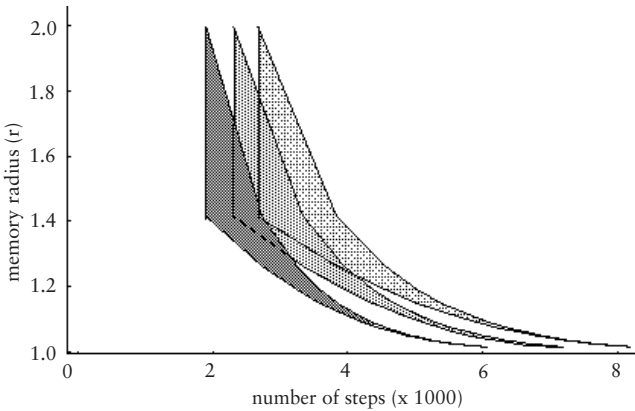

Figure 3. The plot of permitted values for the memory radius r against the number of computer iterations for three different objects' concentrations is shown. The shaded graphs reflect the possible values of the memory radius for a fixed concentration. As the simulations progress the possible domain for the memory radius becomes thinner. The overlap of the permitted values for different concentrations indicates that a RLA will continue to perform a nonoptimized coherent task with a given, possibly wrong, memory radius. This fact shows that the algorithm is stable against local perturbations of the objects' concentration sensed by individual RLA. The concentrations were 5% (I), 10% (II), and 15% (III).

which is valid for $N_\alpha \gg 1$, on the basis of the Euler formula

$$\sum_{i=a}^{b} f(i) \approx \int_{a}^{b} f(x)dx + \frac{1}{2}\left(f(a) + f(b)\right) + \frac{1}{12}\left(f'(b) - f'(a)\right) + \cdots,$$

we have

$$\lambda^{k \to k+1} \approx (2k+1)\frac{\sqrt{N}}{2} \sum_{i=N_\alpha/(k+1)}^{N_\alpha/k} \frac{1}{\sqrt{4i}} \approx 2N(2k+1)\frac{\sqrt{k+1} - \sqrt{k}}{\sqrt{k(k+1)}}.$$

After simplifications we write

$$k \approx \frac{2N}{\lambda}.$$

On the other hand, to build clusters with k objects (in the k-objects steady state sorting stage) the memory radius r must lie in the range $(2^{1/(k+1)}, 2^{1/k})$. Therefore, the last two relations give

$$r \propto \exp\frac{\lambda \ln 2}{2N}. \tag{11}$$

The next step is to design a numerical experiment in order to check our theoretical prediction.

▌ 3.2 Numerical results and the annealing rule

Computation with the functional self-organization algorithm described (see [20–23] for details) requires a well-defined measure of the aggregation stage. Our choice is a texture analysis using features which consider that texture-context information is contained in the overall spatial relationship between its gray tones [29–31]. Let $p(i, j)$ denote the normalized matrix of relative frequencies with which two cells, separated by distance d, occur on the image, one with gray tone i and the other with gray tone j. The matrix of gray-tone spatial-dependence frequencies depends on angular relationships between the neighboring cells. In the following we refer only to the horizontal gray-tone spatial-dependence matrix but arbitrarily oriented matrices can be obtained the same way. We found that the only relevant feature, in this particular numerical experiment, is the *contrast*, which represents a measure of the amount of local variations present in the image

$$\text{contrast} = \sum_{n=0}^{N_g-1} n^2 \left(\sum_{|i-j|=n} p(i, j) \right), \tag{12}$$

where N_g is the number of gray levels present in the image under investigation.
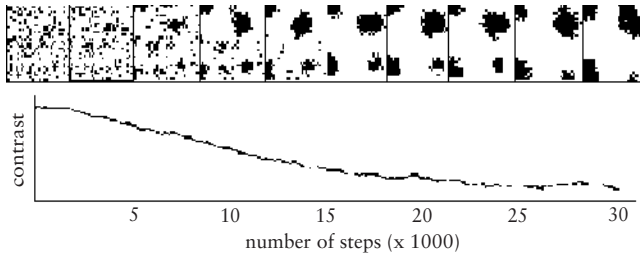
Figure 4. Different snapshots are uniformly sampled with 500 time steps and shown on the top panel. The behavior of the contrast feature against the iteration time step is plotted (lower panel). Here the environment is a rectangular 100×100 lattice, with 10% black object concentration, 40 RLAs, and a constant memory radius $r = 1.1$. As the system approaches its final steady state, the contrast feature saturates. The minimum and maximum values were analytically evaluated and, therefore, can be used to measure the distance between the current aggregation stage and the steady state.

Numerical simulations demonstrate that the defined feature is sensitive to an aggregation stage and offer a quantitative meaning for this fuzzy concept (see Figure 4). Based on the defined global measure, we performed extensive numerical simulations to find the optimal time-dependence of the memory radius r in order to validate the theoretically derived relationship equation (11) and its background hypothesis—the intermediate steady states assumption. We found that at the very beginning of the numerical simulations there is a quasi-linear relationship between the slope of the feature and the time step (see Figure 5). Analyzing Figure 5, we conclude that it is advantageous, in order to reduce the computational effort, to start the numerical simulations with a high value for the memory radius. A high value of the memory radius means a very abrupt decrease of the feature and a rapid slowing-down of the algorithm. If numerical simulation continues along this path, the system needs a long computation time to reach its final steady state. On the other hand, an initial low memory radius determines a slow change in the features but the end of the linear region is closer to its final steady state. Our optimization procedure tries to combine the high speed of the feature decrease for initial high memory radius, with the lowest quasi-steady state at the end of the linear region for a low initial memory radius.

To determine the limits of the linear domain, which means that for a particular value of the memory radius the algorithm enters the slowing down regime, we performed numerical simulations until the linear correlation coefficient is maximum. At that point the final stage of aggregation was reached, for a particular value of the memory radius r. We recorded the slope of the contrast feature for that specific memory
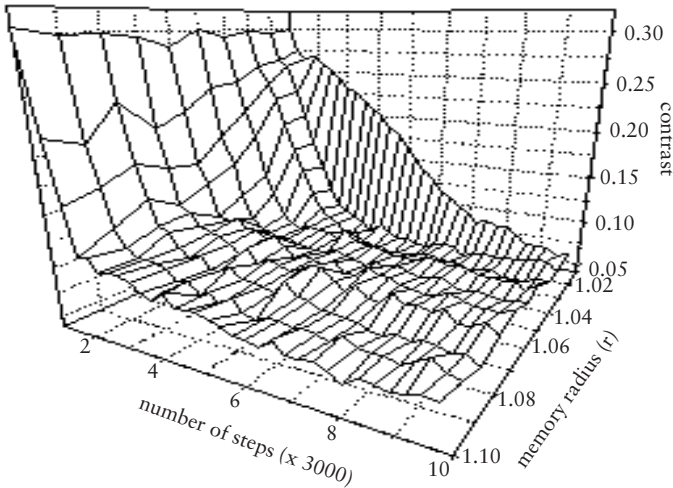
Figure 5. The three-dimensional plot of the contrast feature against the time step and memory radius *r* is shown. With a constant memory radius, a linear dependence of the feature on the time step can be observed at the very beginning of the numerical simulations. Decreases of the memory radius determine a decrease of the slope of the feature. On the other hand, the surfaces are highly fractured and, therefore, an appropriate time-dependent memory radius relationship must be chosen in order to avoid trapping the simulation in a local minimum.

radius value and the simulations were started over for another value of *r*. Figure 6 summarizes the computationally derived optimal relationship between the slope of the contrast feature and the memory radius in order to ensure a minimum computational time. Once the relationship between the microscopic control parameter (memory radius *r*) and the macroscopic measure of aggregation stage (the contrast feature) was established we get a practical instrument with which to optimize the aggregation process.

The computational procedure is as follows. We monitored the slope of the contrast feature and changed the memory radius according to a computationally derived relationship (see Figure 6). The plot of the optimally controlled memory radius against the iteration step (see Figure 7) shows that the interpolation curve (continuous line) agrees with our theoretically derived time-dependent memory radius (see equation (11)).

4. Discussion and conclusions

Previous studies suggested that a realistic approach to the problem of local decision in the aggregation process performed by a team of mobile agents is the first order recurrent memory function [20–23]. The present
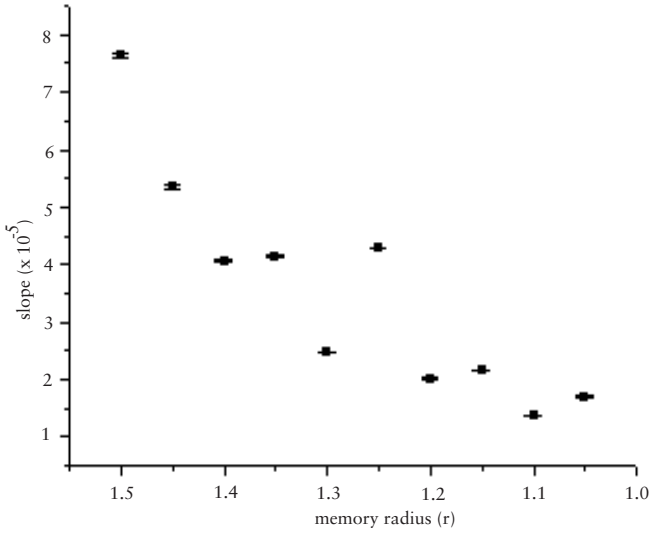
Figure 6. A plot of the steady slope of the contrast feature against the memory radius *r*. The environment is a rectangular 100×100 lattice, with 10% black object concentration and 40 RLAs. The chosen slope of the features maximizes the linear correlation coefficient and, therefore, is an indication that the steady state was reached.
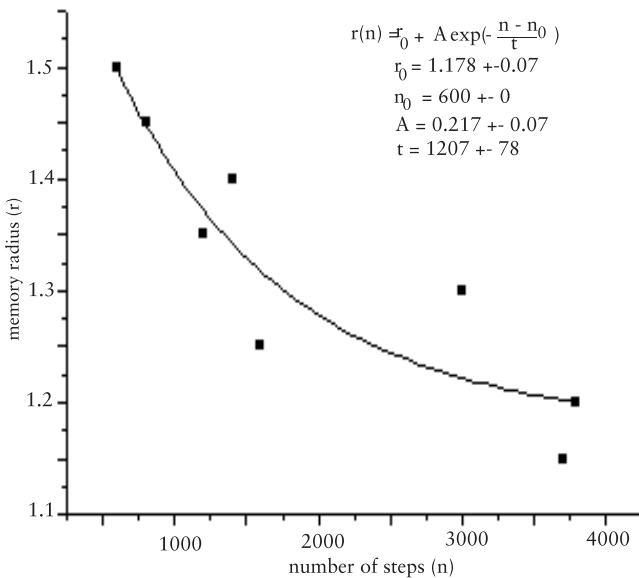

$$r(n) = r_0 + A \exp\left(-\frac{n - n_0}{t}\right)$$
$$r_0 = 1.178 +\!\!-0.07$$
$$n_0 = 600 +\!\!- 0$$
$$A = 0.217 +\!\!- 0.07$$
$$t = 1207 +\!\!- 78$$

Figure 7. The plot of the memory radius *r* against the time step *n* when the sorting steady state was reached. The best fit is an exponentially decaying function with the indicated parameters.

study analyzes the dynamical aspects of the memory feature, particularly, its correlation length or memory radius. Based on the intermediate steady state hypothesis we derived a theoretical time-dependent memory radius that leads to a minimum aggregation time. The intuitive idea behind our approach is that each two-, three-, four-, *etcetera* object clusters are metastable and the inherent stochastic behavior of the robot-like-ants (RLAs) is the mechanism that drives the systems from intermediate (metastable) steady states to a final (stable) steady state. Once we found a time-dependent memory radius, which we thought to be the optimum, the next step was to check our finding using numerical simulation.

We used the contrast feature as a quantitative measure to characterize the global dynamics of the cluster aggregation. The choice of this specific feature is particularly important in the case of optimization of the algorithm. This feature allows comparison between different speeds of aggregation. The speed of saturation of the contrast feature strongly depends on the control parameter (memory radius). Therefore, it was used as an optimization criterion for the computational implementation. Based on this computational optimization criterion we were able to derive a relationship between the memory radius r and the iteration step. The agreement between the theoretically derived relationship and the numerically derived relationship based on maximization of the contrast feature speed is satisfactory.

It is questionable whether the contrast feature is a relevant measure of the clustering process. We found that other texture features available in the field of image processing (angular second-momentum, correlation, etc.) might present relevant dependencies on the control parameter (memory radius). However, our preliminary results indicate that for the very simple behavior we studied (sorting and clustering) using the speed of variation of the other features as an optimization criterion does not change the annealing law.

The self-organization approach is widespread because the same individual level behaviors may be used to generate different collective responses in different environments. For example, a combination of computer simulations and field experiments show in [3] that the different exploratory patterns of army ants species could result from different spatial distributions of their prey and not necessarily from differences in individual behaviors. These simulations do not imply that individuals of all species of army ants have exactly the same behavior, but suggest that behavioral rules may be qualitatively similar in all species, possibly because of common ancestors: evolution may then have modulated these rules quantitatively (by changing response thresholds or specific chemicals). It appears therefore that self-organization may have been favored by evolution since it facilitates the emergence of efficient collective patterns and does not require complex individuals. However, the

question of how self-organization and evolution interact is still largely open, not only in insect societies but also in ecology, ethnology, and biology in general [32].

On the other hand, using a swarm of robots inspired by social insect behavior has some drawbacks. For example, stagnation is one: because of the lack of a global knowledge, a group of robots may find itself in a deadlock, where it cannot make any progress. Another problem is to determine how these so-called "simple" robots should be programmed to perform user-designed tasks. The pathways to solutions are usually not predefined but emergent, and solving a problem amounts to finding a trajectory for the system and its environment so that the states of both the system and the environment constitute the solution to the problem. Although appealing, this formulation does not lend itself to easy programming. Until now, we implicitly assumed that all robots were identical units. The situation becomes more complicated when the robots have different characteristics, respond to different stimuli, or respond differently to the same stimuli, and so forth. If the body of theory that roboticists can use for homogeneous groups of robots is limited, there is virtually no theoretical guideline for the emergent design and control of heterogeneous swarms.

Appendix

The goal of this appendix is to derive the maximum and minimum values for global measure of the aggregation—the contrast. To simplify the evaluations, only the case of a two-dimensional lattice environment is discussed. We assumed that three object types denoted by a, b, and respectively, ϕ (empty site) are present. Let $N_{int}(i)$ be the lattice site number inside the i-type object cluster and $N_{ext}(i)$ the bordering lattice site number for the same cluster (see Figure 8). Considering only the nearest neighbor interaction, a rough estimation of the spatial-dependence matrix entries is

$$p(i, i) = \frac{1}{N} \left(2N_{int}(i) + \left(N_{ext}(i) \right)_x \right), \tag{A.1}$$

where N is a normalization factor and $(N_{ext}(i))_x$ is the number of bordering lattice sites of the i type cluster in the horizontal direction. For symmetric clusters this number is

$$\left(N_{ext}(i) \right)_x \approx \left(N_{ext}(i) \right)_y = \frac{1}{2} N_{ext}(i).$$

To carry out algebraic manipulations we adopted a numerical equivalence for the object types $(a, b, \phi) \to (1, 2, 3)$. Moreover, we assumed that the a type object clusters and the b type object clusters do not overlap. Under such assumptions
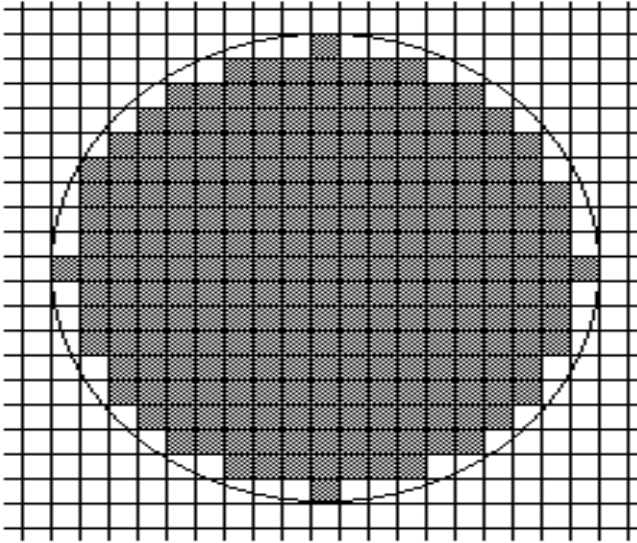
$$p(1, 2) = p(2, 1) = 0,$$

Figure 8. Symmetric cluster of *a* type objects (black pixels) in the two-dimensional rectangular lattice. This was found numerically to be the most probable steady state of sorting.

$$p(1,3) = p(3,1) = \frac{1}{N}\left(N_{\text{ext}}(1)\right)_x$$
$$p(2,3) = p(3,2) = \frac{1}{N}\left(N_{\text{ext}}(2)\right)_x. \tag{A.2}$$

Using equations (A.1) and (A.2), the matrix of a symmetric pattern (see Figure 8) writes

$$(P) =$$
$$\frac{1}{N}\begin{pmatrix} 2N(1) - \frac{3}{2}N_{\text{ext}}(1) & 0 & \frac{1}{2}N_{\text{ext}}(1) \\ 0 & 2N(2) - \frac{3}{2}N_{\text{ext}}(2) & \frac{1}{2}N_{\text{ext}}(2) \\ \frac{1}{2}N_{\text{ext}}(1) & \frac{1}{2}N_{\text{ext}}(2) & 2N(3) - \frac{3}{2}N_{\text{ext}}(3) \end{pmatrix}, \tag{A.3}$$

where

$$N = 2(N(1) + N(2) + N(3)) - \frac{1}{2}(N_{\text{ext}}(1) + N_{\text{ext}}(2)) - \frac{3}{2}N_{\text{ext}}(3). \tag{A.4}$$

The conservation rule writes

$$N_{\text{ext}}(3) = N_{\text{ext}}(1) + N_{\text{ext}}(2)$$
$$N(1) + N(2) + N(3) = N_x N_y \tag{A.5}$$

where N_x (N_y) is the total number of horizontal (vertical) lattice sites. Using equations (A.4) and (A.5) results in

$$N = 2\left[N_x N_y - \left(N_{\text{ext}}(1) + N_{\text{ext}}(2)\right)\right].$$

Let us denote the concentration of the i type objects by

$$c_i = \frac{N(i)}{N_x N_y}.$$

If the cluster dimension $N(i)$ is big enough then a rough estimation for the number of bordering sites is $N_{\text{ext}}(i) \approx \alpha\sqrt{N(i)}$, where $\alpha \in (0, 1)$ is a constant. Substituting this into equation (A.3), one obtains

$$N \approx 2N_x N_y \left[1 - \alpha \frac{\sqrt{N(1)} + \sqrt{N(2)}}{N_x N_y}\right]$$

$$= 2N_x N_y \left[1 - \alpha \left(\sqrt{\frac{c_1}{N_x N_y}} + \sqrt{\frac{c_2}{N_x N_y}}\right)\right]. \tag{A.6}$$

Substituting equation (A.6) into (A.3), and using the notation $y = \alpha/\sqrt{N_x N_y}$, matrix (P) becomes:

$(P) =$

$$\frac{1}{1 - y\left(\sqrt{c_1} + \sqrt{c_2}\right)} \begin{pmatrix} c_1 - \frac{3}{4}y\sqrt{c_1} & 0 & \frac{y}{2}\sqrt{c_1} \\ 0 & c_2 - \frac{3}{4}y\sqrt{c_2} & \frac{y}{2}\sqrt{c_2} \\ \frac{y}{2}\sqrt{c_1} & \frac{y}{2}\sqrt{c_2} & c_3 - \frac{3}{4}y\sqrt{c_3} \end{pmatrix}, \tag{A.7}$$

where the conservation law $c_1 + c_2 + c_3 = 1$ was used. Based on equations (12) and (A.8) one finds

$$\text{contrast} = \sum_{n=0}^{2} n^2 \left(\sum_{i,j;|i-j|=0}^{3} p(i,j)\right) = \frac{y\left(2\sqrt{c_1} + \sqrt{c_2}\right)}{1 - y\left(\sqrt{c_1} + \sqrt{c_2}\right)}.$$

A major, realistic, simplification is $y \ll 1$, which means that the lattice is either big enough or is periodic in order to avoid the edge effects. Another major simplification is $c_1 = c_2 = c$, meaning that the two object types have equal concentration. Under these assumptions, the contrast feature can be written

$$\text{contrast} \approx 5y\sqrt{c}\left(1 + 2y\sqrt{c}\right) \quad => \lim_{y \to 0} \text{contrast} = 0.$$

The last two simplified values for the contrast feature were obtained for the final stage of the aggregation process.

   To complete the analytical description of the aggregation process by global features the above features must be evaluated for the initial (noisy) configuration. To this purpose, let us denote by $N(i,j)$ the number of $i - j$ nearest neighbor sites. According to our previous assumptions

$$N(1, 1) = N(2, 2) = 0,$$
$$N(1, 2) + N(1, 3) = 2N(1),$$
$$N(2, 1) + N(2, 3) = 2N(2),$$
$$N(3, 1) + N(3, 2) + N(3, 3) = 2N(3). \tag{A.8}$$

From a geometric point of view it is straightforward that $N(3, 1) + N(3, 2) \propto \sqrt{N(3)}$. Due to high symmetry in the noisy configuration we can assume that:

$$
\begin{aligned}
N(1, 2) &= N(2, 1) = N_{12}, \\
N(1, 3) &= N(3, 1) = N_{13}, \\
N(2, 3) &= N(3, 2) = N_{23}.
\end{aligned}
\tag{A.9}
$$

Using equations (A.8) and (A.9) results in

$$
\begin{aligned}
N_{12} &= N(1) + N(2) - \frac{\beta}{2}\sqrt{N(3)}, \\[4pt]
N_{13} &= N(1) - N(2) + \frac{\beta}{2}\sqrt{N(3)}, \\[4pt]
N_{23} &= -N(1) + N(2) + \frac{\beta}{2}\sqrt{N(3)}, \\[4pt]
N_{33} &= 2N(3) - \beta\sqrt{N(3)},
\end{aligned}
$$

where $\beta \in (0, 1)$ is a constant. Therefore, by considering $N = 2N_x N_y$, the corresponding matrix of the noisy pattern is

$$
(P) = \frac{1}{N}
\begin{pmatrix}
0 & c_1 + c_2 - \frac{\beta}{2}\sqrt{\frac{c_3}{N_x N_y}} & c_1 - c_2 + \frac{\beta}{2}\sqrt{\frac{c_3}{N_x N_y}} \\
c_1 + c_2 - \frac{\beta}{2}\sqrt{\frac{c_3}{N_x N_y}} & 0 & -c_1 + c_2 + \frac{\beta}{2}\sqrt{\frac{c_3}{N_x N_y}} \\
c_1 - c_2 - \frac{\beta}{2}\sqrt{\frac{c_3}{N_x N_y}} & -c_1 + c_2 + \frac{\beta}{2}\sqrt{\frac{c_3}{N_x N_y}} & 2c_3 - \beta\sqrt{\frac{c_3}{N_x N_y}}
\end{pmatrix}.
$$

If the lattice environment is large enough or periodic the matrix (P) becomes

$$
(P) = \frac{1}{N}
\begin{pmatrix}
0 & c_1 + c_2 & c_1 - c_2 \\
c_1 + c_2 & 0 & -c_1 + c_2 \\
c_1 - c_2 & -c_1 + c_2 & 2c_3
\end{pmatrix}.
$$

In the limit case considered above $(\beta\sqrt{c_3/N_x N_y} \to 0)$ the contrast features are

$$
\text{contrast} \approx 2c.
$$

References

[1] G. Nicolis and I. Prigogine, *Self-organization in Non-equilibrium Systems* (Wiley, New York, 1997).

[2] J.-L. Deneubourg and S. Goss, "Collective Patterns and Decision Making," *Ethology, Ecology and Evolution*, **1** (1989) 295–311.

[3] N. R. Franks, "The Blind Leading the Blind in Army Ant Raid Patterns: Testing a Model of Self-organization," *Journal of Insect Behaviour*, **4** (1991) 583–607.

[4] R. Beckers, J.-L. Deneubourg, and S. Goss, "Trails and U-turns in the Selection of a Path by the Ant Lasius Niger," *Journal of Theoretical Biology*, **159** (1992) 397–415.

[5] L. Edelstein-Keshet, J. Watmough, and G. B. Ermentrout, "Trail Following in Ants: Individual Properties Determine Population Behavior," *Behavioral Ecology and Sociobiology*, **36** (1995) 119–133.

[6] N. R. Franks, S. Bryant, R. Griffiths, and L. Hemerik, "Synchronization of the Behaviour within Nests of the Ant Leptothorax Acervorum (Fabricius): I. Discovering the Phenomenon and its Relation to the Level of Starvation," *Bulletin of Mathematical Biology*, **52** (1990) 597–612.

[7] B. J. Cole, "Short-term Activity Cycles in Ants: Generation of Periodicity by Worker Interaction," *The American Naturalist*, **137** (1991) 244–259.

[8] J. Watmough and S. Camazine, "Thermoregulation of Honeybee Clusters," *Journal of Theoretical Biology*, **176** (1995) 391–402.

[9] J.-L. Deneubourg, S. Gross, N. Franks, A. Sandova-Franks, C. Detrian, and L. Chretien, "The Dynamics of Collective Sorting: Robot-like Ant and Ant-like Robot," in *From Animals to Animats: Proceedings of the First International Conference on Simulation of Adaptive Behavior*, edited by J. A. Meyer and S. W. Wilson (MIT Press, 1991).

[10] I. Karsai, Z. Penzes, and J. W. Wenzel, "Dynamics of Colony Development in Polistes Dominulus: A Modeling Approach," *Behavioral Ecology and Sociobiology*, **39** (1996) 97–105.

[11] P. Hogeweg and B. Hesper, "Socioinformatic Processes: MIRROR Modelling Methodology," *Journal of Theoretical Biology*, **113** (1985) 311–330.

[12] G. Theraulaz, S. Goss, J. Gervet, and J.-L. Deneubourg, "Task Differentiation in Polistes Wasp Colonies: A Model for Self-organizing Groups of Robots," in *From Animals to Animats: Proceedings of the First International Conference on Simulation of Adaptive Behavior*, edited by J. A. Meyer and S. W. Wilson (MIT Press, 1991).

[13] G. Theraulaz, J. Gervet, and S. Semenoff-Tian-Chansky, "Social Regulation of Foraging Activities in Polistes Dominulus Christ: A Systemic Approach to Behavioural Organization," *Behaviour*, **116** (1991) 292–320.

[14] S. W. Pacala, D. M. Gordon, and H. C. J. Godfray, "Effects of Social Group Size on Information Transfer and Task Allocation," *Evolutionary Ecology*, **10** (1996) 127–165.

[15] C. Tofts and N. R. Franks, "Foraging for Work: How Tasks Allocate Workers," *Animal Behaviour*, **48** (1994) 470–472.

[16] Y. U. Cao, A. S. Fukunaga, and A. B. Kahng, "Cooperative Mobile Robotics: Antecedents and Directions," *Autonomous Robots*, **4** (1997) 1–23.

[17] Rodney A. Brooks, "A Robust Layered Control System for a Mobile Robot," *IEEE Journal of Robotics and Automation*, **RA-2** (1986) 14–23.

[18] P. Caloud, W. Choi, J. C. Latombe, C. Le Pape, and M. Yim, "Indoor Automation with Many Mobile Robots," *IEEE/RSJ International Conference on Intelligent Robots and Systems*, (1990) 67–72.

[19] R. Chauvin, "Sur le transport collectif des proies par Formica polyctena," *Insectes Sociaux*, **25** (1968) 193–200.

[20] S. A. Oprisan, V. Holban, and B. Moldoveanu, "Functional Self-organization Performing Wide-sense Stochastic Processes," *Physics Letters A*, **216** (1996) 303–306.

[21] S. A. Oprisan, "Convergence Properties of the Functional Self-organization Stochastic Algorithm," *Journal of Physics A: Mathematical and General*, **31** (1998) 8451–8463.

[22] D. Amarie, S. A. Oprisan, and M. Ignat, "Random Walk Systems Behavior Based on Record Function," *Physics Letters A*, **254** (1999) 112–118.

[23] C. V. Giuraniuc and S. A. Oprisan, "Short Range and Long Range Coupling in Stochastic Functional Self Organization," *Physics Letters A*, **259** (1999) 334–338.

[24] S. A. Oprisan, A. Ardelean, and P. T. Frangopol, "Self-organization and Competition in the Immune Response to Cancer Invasion. A Phase-orientated Computational Model of Oncogenesis," *Bioinformatics*, **60** (2000) 1–5.

[25] J. von Neumann, in *Theory of Self-Reproducing Automata*, edited by A. W. Burks (University of Illinois Press, Urbana, 1966).

[26] J. von Neumann, in *Essays on Cellular Automata*, edited by A. Burks (University of Illinois Press, Urbana, 1970).

[27] N. Boccara, E. Goles, S. Martinez, and P. Picco (editors), *Cellular Automata and Cooperative Systems* (Kluwer Academic, Dorderecht, 1993).

[28] J. M. Perdang and A. Lejeune, *Cellular Automata* (World Scientific, Singapore, 1993).

[29] R. Haralick, K. Shanmugan, and I. Distein, "Textural Features for Image Classification," *IEEE Transactions on Systems, Man and Cybernetics*, **3** (1973) 610–621.

[30] S. Blacher, F. Brouers, and G. Ananthakrishna, "Multifractal Analysis, a Method to Investigate the Morphology of Materials," *Physica A*, **185** (1992) 28–40.

[31] S. Blacher, F. Brouers, R. Fayt, and P. Teyssie, "Multifractal Analysis: A New Method for the Characterization of the Morphology of Multicomponent Polymer Systems," *Journal of Polymer Science: Part B: Polymer Physics*, **31** (1993) 655–670.

[32] S. A. Kauffman, *The Origins of Order* (Oxford University Press, Oxford, 1993).